Chapter 3
Basic Ultrasound Physics, Doppler Ultrasound, and Hemodynamic Assessment

Gerard R. Manecke, MD

Abstract A basic understanding of physics is necessary for effective clinical use of ultrasound, and it allows appreciation of the wonderful technology we now use. Rapid waveform analysis and massive data storage capability make high-resolution imaging and complex hemodynamic assessment accessible at the bedside. Understanding the principles of ultrasound physics and applying them to echocardiography help us to understand the anatomy and function of the heart, while use of Doppler principles allows us to make assessments of blood flow, valve areas, and pressure gradients.

Keywords Transesophageal echocardiography · Ultrasound physics · Doppler principles · Doppler ultrasound · Hemodynamic assessment

Basic Ultrasound Physics

Some animals make use of sound wave reflections to determine their position and direction of motion (echolocation) [1, 2]. Bats, with their poor vision, transmit ultrasonic signals and are particularly adept at echolocation [3, 4]. Visually impaired humans can develop similar capabilities using audible sound, resulting in an impressive ability to navigate surroundings [5, 6]. Ultrasound in the form of Sound Navigation and Ranging (SONAR) was developed in early twentieth century, and was first employed for military purposes shortly after the First World War [7]. Medical ultrasound was first introduced by George Ludwig in 1949 [8] and cardiac ultrasound was first employed in 1953 [9]. An explosion in computer technology in the 1980s allowed the development of two-dimensional (2D) ultrasound for continuous imaging, Doppler blood flow, and tissue movement measurements. Further advances in computer technology provide the high-resolution

G.R. Manecke, MD (✉)
Department of Anesthesiology, University of California San Diego, 200 West Arbor Drive, MC 8770, San Diego, CA, USA
e-mail: gmanecke@ucsd.edu

T.M. Maus et al. (eds.), *Essential Echocardiography*,
DOI 10.1007/978-3-319-34124-8_3

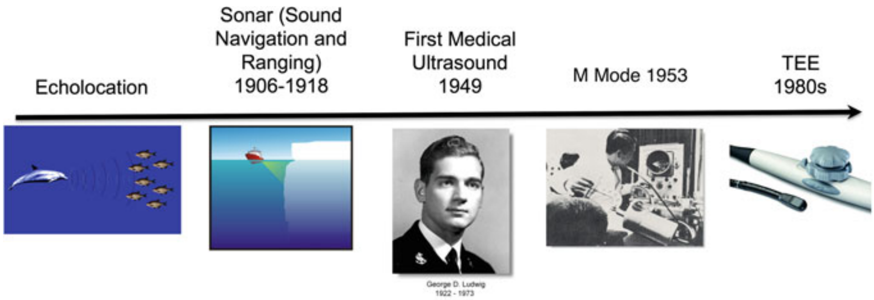

Fig. 3.1 Timeline of the history of ultrasound

Fig. 3.2 Characteristics of sound waves. *F* frequency, *P* Period

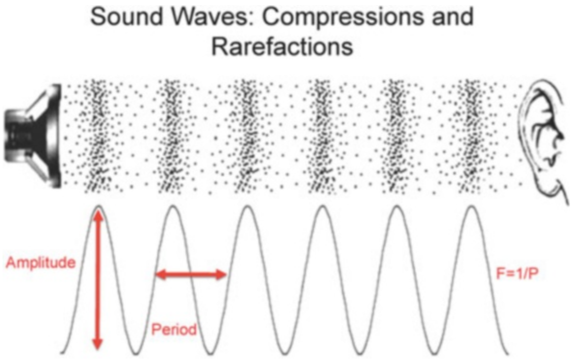

three-dimensional imaging with continuous display we currently enjoy [10]. A timeline of the history of ultrasound is shown in Fig. 3.1.

Physics of Ultrasound

Sound waves are pressure waves: compressions and rarefactions of the molecules occur in the medium in which they are traveling. Like all waves, sound waves have amplitude (loudness) and frequency (pitch) (Fig. 3.2). Humans can hear sounds within the range of 20–20,000 cycles per second (Hz). Ultrasound is sound at frequencies above the audible range (>20,000 Hz), while medical ultrasound is in the mega-Hz (MHz) range, or millions of Hz (Fig. 3.3).

Sound transmission depends upon the density of the medium, with higher density substances such as liquid transmitting sound more rapidly and efficiently than air. Ultrasound does not travel well through gas, so gas-filled spaces such as bronchi and gastric air result in "blackout" of the ultrasound image. Lower frequency sound tends to propagate farther than high frequency sound. One notices this when a storm is approaching. When the storm is distant, thunder sounds like a

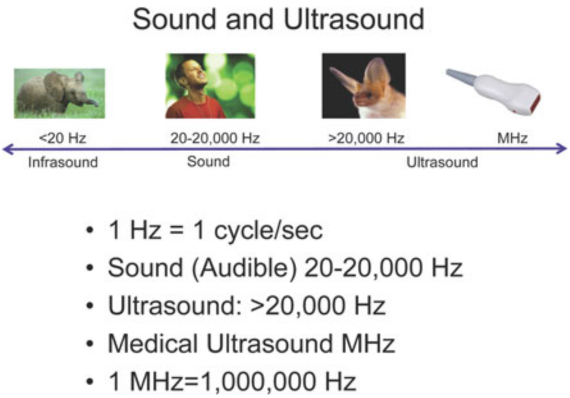

Fig. 3.3 Sound frequencies. Medical ultrasound is in the Mega-Hz (million Hz) range

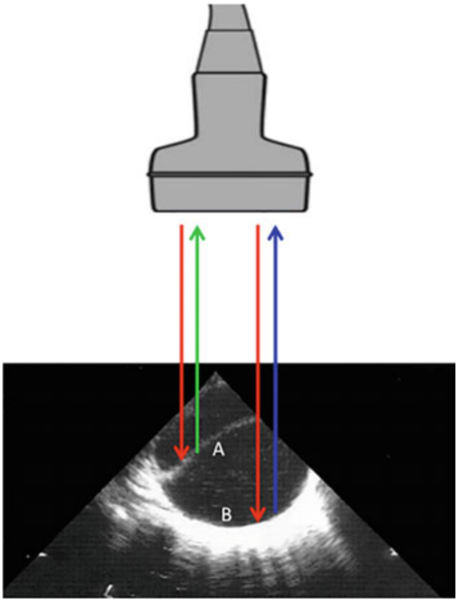

Fig. 3.4 "Specular Echoes." Ultrasound waves bouncing off tissues of varying density, *A* is the intimal flap of an aortic dissection, *B* is the distal wall of the aorta

low-pitched "rumble." As the storm approaches, the sound of thunder includes higher frequencies, resulting in a "thunder clap." Ultrasound behaves similarly, so imaging objects distant from the transducer requires lower frequencies than imaging close objects.

When sound waves strike an interface of a different density, they bounce off that interface. This is the principle upon which two-dimensional ultrasound is based [11]. The ultrasound transducer emits ultrasound, the ultrasound bounces off a density interface (object) back to the transducer, and the time required allows calculation of the distance the object is from the transducer. As demonstrated in

Fig. 3.4, a cross-sectional image of the descending aorta shows ultrasound waves bouncing off of two density interfaces: a dissection intimal flap (*A*) and the distal wall of the aorta (*B*). A perpendicular orientation of the object to the ultrasound probe is optimal for return of echo signals. A parallel orientation may not provide a sufficient reflection of signals, leading to drop out.

Ultrasound Probes

Ultrasound probes have both emission and sensing capabilities. Each probe contains an array of pressure-electric (piezoelectric) crystals that convert electrical energy to pressure waves (for emitting ultrasound) and pressure waves to electricity (for sensing). The lateral resolution of the image depends upon the distance between the crystals aligned within the probe, with a smaller distance associated with better resolution (Fig. 3.5). The lateral resolution may also be altered by focusing. Akin to utilizing a magnifying glass in the sunshine to focus the sunlight into a narrow beam, modern ultrasound machines have an adjustable focal point that represents the narrowest part of the beam (Fig. 3.6). Lateral resolution is best at the focal point, but is quite poor in the far field (distal to the focal point). Therefore, it is recommended to place the focal point at the level of the structure of interest.

The longitudinal, or axial resolution depends on the pulse length, with shorter pulse length resulting in better resolution (Fig. 3.7). Pulse length can be decreased either by increasing the frequency of the probe (and thus decreasing the wavelength), or decreasing the cycles/pulse Eq. 3.1 and Eq. 3.2. Higher frequency probes with shorter wavelengths thus have better resolution Eq. 3.3. Note that resolution is expressed as distance, so a *lower* number indicates *better* resolution.

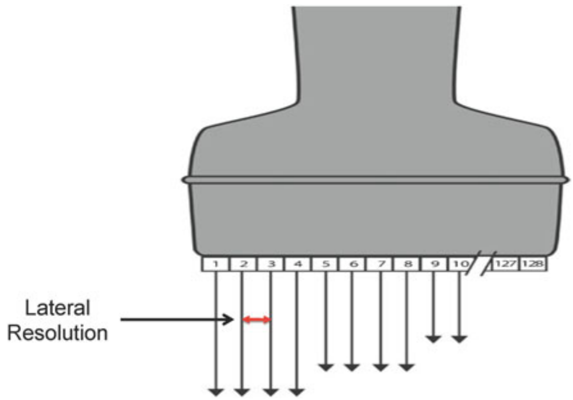

Fig. 3.5 Lateral resolution depends upon the distance between piezoelectric crystals in the probe

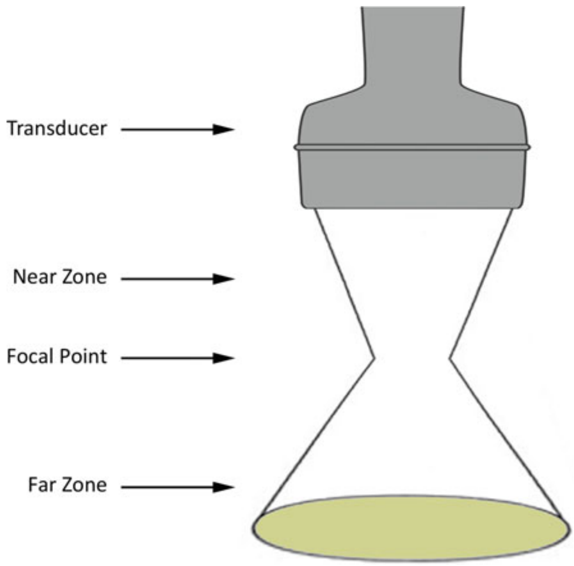

Fig. 3.6 Focus influence on beam width. The narrowest portion of the beam is at the focal point with poorer resolution in the far zone

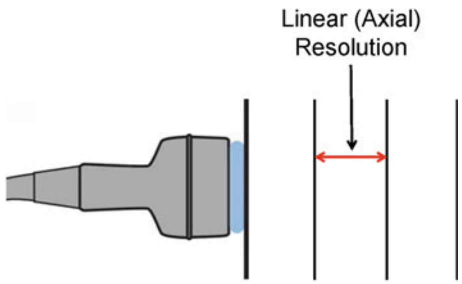

Fig. 3.7 Axial resolution depends upon the pulse length and the probe frequency

$$\text{Frequency} = 1/\text{wavelength} \tag{3.1}$$

$$\text{Pulse length} = \text{wavelength} \times \text{cycles/pulse} \tag{3.2}$$

$$\text{Axial Resolution} = \frac{0.77 \times \frac{\text{cycles}}{\text{pulse}}}{\text{Frequency}} \tag{3.3}$$

The effects of probe frequency on ultrasound imaging are summarized in Table 3.1, with the general rule that distant objects can be viewed best using a low frequency probe, however, the resolution will be poorer at the lower frequency. Likewise, small objects close to the probe, such as the radial artery with surface ultrasound, are best visualized using a high frequency probe because of the associated high resolution. The trade-off of high frequency imaging is the inability to visualize deeper structures due to energy dissipation.

Table 3.1 The effects of probe frequency on ultrasound imaging

• **High frequency**
– More energy dissipation – Better linear resolution – Close objects with high resolution
• **Low frequency**
– Less energy dissipation – Poor linear resolution – Far objects viewed but less resolution

While lateral and axial resolution represent the spatial resolutions of ultrasound, cardiac ultrasound requires interpreting moving clips as opposed to still images. Therefore, one must consider temporal resolution. This is similar to movie and television images where at an analog movie theater one would note a flickering of the image, however, at home on a television there is no longer a flickering of the image. With modern televisions, the high-definition frame rate is high enough such that even fast moving objects (e.g., sporting events) appear smoothly. This is due to the improved frame rate moving from analog movie theater to television to high-definition television.

With ultrasound, the machine has to produce numerous ultrasound pulses in a fan-like fashion to develop one single image. Repeating this process will provide subsequent images yielding a moving clip. The number of images developed per second is termed the frame rate. The more imaging (e.g., deeper or wider) and processing (e.g., color flow Doppler in addition to 2D) that a machine is requested to do, the longer it will take to generate a single image, subsequently reducing the frame rate. If the frame rate is too slow, the video will begin to appear choppy or flip-book like, reducing the ability to detect fine cardiac movement. Therefore, only the depth needed and the color flow Doppler box size needed should be utilized to maintain the best frame rate.

Doppler Ultrasound

In 1842, Austrian physicist Christian Doppler postulated that the difference in color between double stars could be explained by their motion. The effect of an object's motion on the frequency of waves detected from it is known as the "Doppler Effect." An example of the Doppler effect is the change in pitch of a train whistle as the train passes by an observer. This principle is applied in ultrasound with blood flow velocity measurements as illustrated in Fig. 3.8. Ultrasound at a known frequency (f_T) is transmitted from the probe, bounces off a moving object (blood cells), and the reflected sound is detected by the probe. The frequency of the returning ultrasound (f_r) is calculated, and the frequency shift between the transmitted and returning ultrasound (Δf) is used to calculate the velocity of blood flow (V):

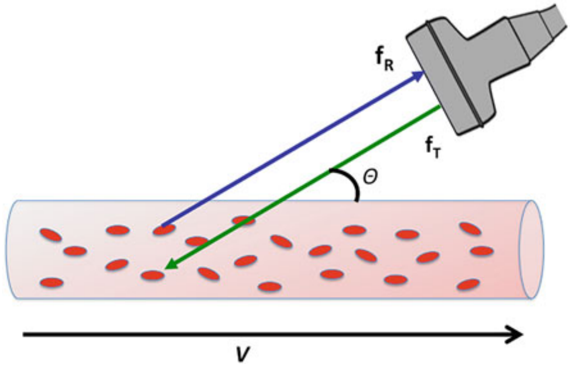

Fig. 3.8 Doppler assessment of blood flow velocity. The closer the alignment of blood flow with the Doppler beam (angle $\Theta = 0$), the more accurate the result. V is blood flow velocity, f_T is transmitted frequency (known), F_R is the returning frequency (calculated). The difference between f_T and F_R is the frequency shift, Δf

$$V = \frac{C(\Delta f)}{2f_T \cos\theta} \tag{3.4}$$

V = velocity of blood flow, C = speed of sound, Δf = frequency shift (difference between transmitted and received frequency), Θ = angle between blood flow path and Doppler beam.

Closer alignment of the blood flow and the Doppler beam (Θ) yields a more accurate measurement (cos 0° = 1). Of note, the cos 90° = 0 and therefore, measurement of flow perpendicular to the probe cannot be calculated. As opposed to 2D imaging which prefers the object to be perpendicular to the probe, Doppler imaging prefers the object to be parallel in orientation.

The Doppler Principle is used clinically in three ways: color flow Doppler (CFD), pulse wave Doppler (PWD), and continuous wave Doppler (CWD). CFD results in a real-time color flow diagram, PWD determines the velocity at a discrete area in space ("sample volume"), and CWD determines flow velocity along an axis. Tissue Doppler is simply a variation of PWD, used to determine the velocity of tissue movement (e.g., the mitral annulus) as opposed to blood movement. The characteristics, uses, and limitations of Doppler techniques are summarized in Table 3.2.

An important and sometimes useful artifact is *aliasing*. Aliasing is a false frequency wave or image resulting when the sampling rate of the sensor is too low to

Table 3.2 Characteristics and clinical use of Doppler techniques

	Color flow Doppler	Pulse wave Doppler	Continuous wave Doppler
Color map	+	–	–
Assess flow at a discrete area	+	+	–
Assess flow along an axis	–	–	+
Qualitative assessment	**Very useful**	Useful	Less useful
Quantitative assessment high flow	Less useful	Less useful	**Very useful**
Aliasing	+	+	–

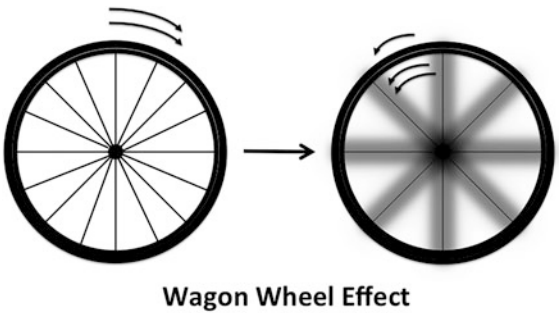

Fig. 3.9 "Wagon Wheel Effect." Rapid movement of spokes is interpreted as slow moving, large "blurred" spokes, often in the opposite direction

accurately detect the high frequency of the returning signal. The *Nyquist Theorem* states that the sampling rate must be at least twice the frequency of the wave being sampled. The *Nyquist Limit* is the highest frequency that can be accurately sampled at a given sampling rate. Aliasing is often called the "Stroboscopic" or "Wagon Wheel" effect, in which rapidly moving spokes of a wheel in one direction appear as slow moving blurred spokes (Fig. 3.9, https://www.youtube.com/watch?v=jHS9JGkEOmA). This results from either, in a video, the frame rate being too slow to pick up the actual speed of the spokes, or in real time, the inability of the human central nervous system to process the fast spoke motion. If the "snapshots" (samples) of the moving spokes are not frequent enough, the spokes appear to be moving slowly, sometimes in the opposite direction.

After transmitting an ultrasound wave, the probe "samples" the returning wave. In CFD and PWD, the probe "waits" until a transmitted signal bounces off the target and is received, so the sampling rate is limited by this process. Aliasing thus results if the returning frequency is higher than half the sampling rate. In CWD, the sampling and transmission are simultaneous—the probe does not wait for the returning signal, so aliasing does not occur. CWD is thus preferred for measurement of high velocity (high returning frequency) flow. Aliasing results in the "wrap around" appearance of PWD tracings (Fig. 3.10) and the appearance of flow in the opposite direction of the actual flow in CFD (Fig. 3.11). The latter may be useful, since the velocity at which aliasing occurs is known and can be applied to calculations such as Proximal Isovelocity Surface Area (PISA) [12].

Hemodynamic Assessment

Echocardiography can be used for an accurate assessment of hemodynamics. The most common applications are quantifications of flow, valvular area, and pressure gradients.

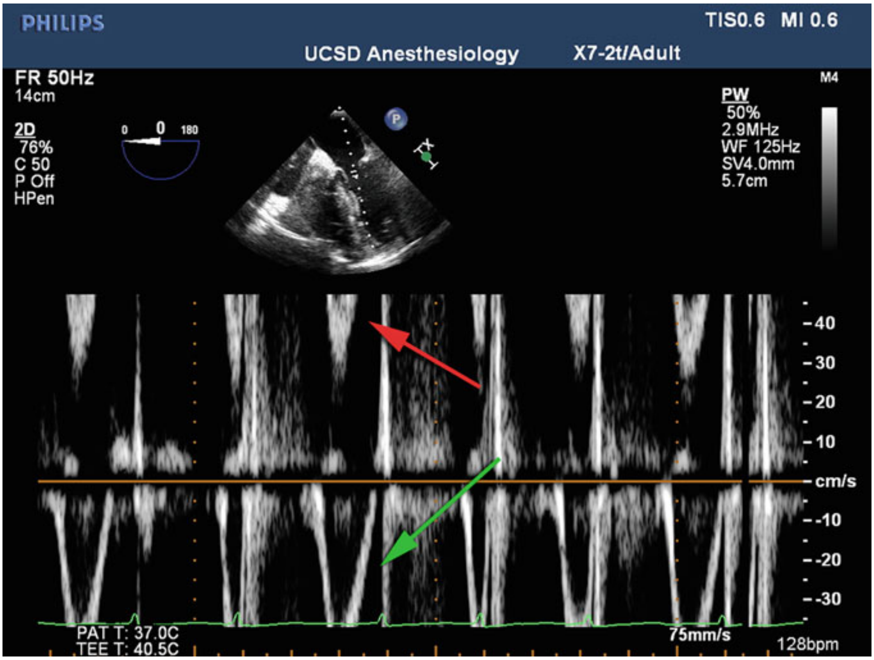

Fig. 3.10 Pulse Wave Doppler of transmitral flow. Flow away from the transducer is displayed as below the zero line. Flow becomes so rapid (*green arrow*) that it is displayed as flow in the opposite direction (*red arrow*, "Wrap Around")

Flow

Blood flow measurement is typically utilized in determining stroke volume and subsequently cardiac output. A stroke volume is determined by calculating the cross-sectional area of the blood vessel and multiplying it by the area under the Doppler velocity–time curve. The area under the Doppler velocity–time curve is called the "Velocity Time Integral" (VTI), or the "Stroke Distance." Figure 3.12a explains how the area under the curve provides a distance by plotting velocity and time of a traveling car. In the example, a car traveling at 75 miles per hour for 2 h will have traveled a distance of 150 miles (analogous to "Stroke Distance"). The cross-sectional area of the blood vessel is estimated by determining the radius of the vessel (diameter divided by 2) and assuming the shape is circular (area = πr^2) (Fig. 3.12b).

$$\text{Stroke Volume} = \text{Area} * \text{VTI} \tag{3.5}$$

For example, to calculate the left ventricular stroke volume, one can measure the diameter of the left ventricular outflow tract (LVOT) using the midesophageal aortic valve long axis view (Fig. 3.13a), with Area = $\pi(D/2)^{2.}$ Using the deep

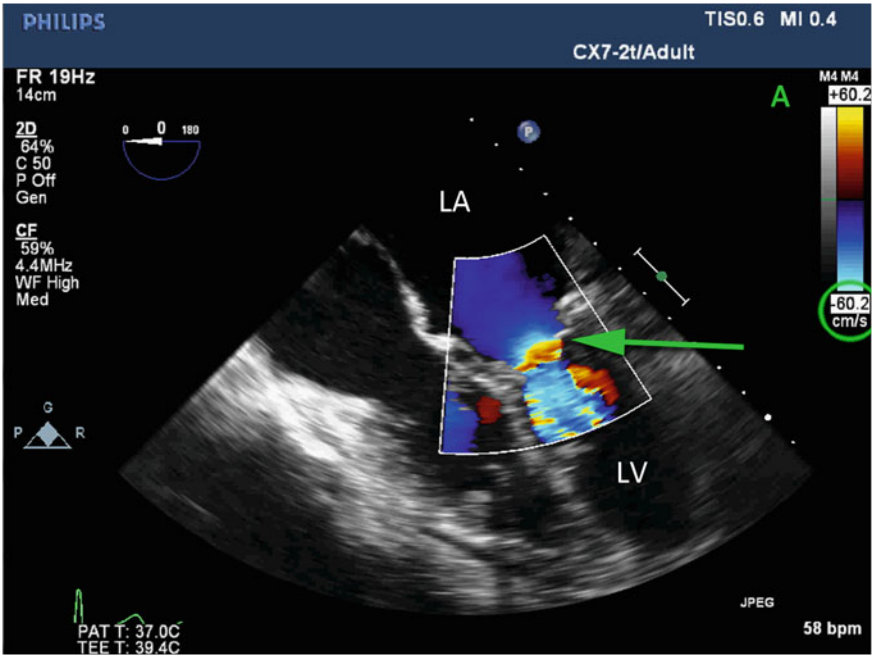

Fig. 3.11 Midesophageal four-chamber view with transmitral color flow Doppler demonstrating aliasing. The flow map (*A*) indicates that flow away from the probe is *blue*, flow toward the probe is *yellow*, and the limit below which aliasing does not occur is 60.2 cm/sec. The *arrow* shows an aliasing line, where flow exceeds 60.2 cm/sec, and downward flow turns from *blue* to *yellow*. *LA* left atrium; *LV* left ventricle

transgastric long axis view, CWD can be used to obtain the LVOT systolic Doppler wave, and the VTI can be determined by tracing the wave. Stroke volume is then calculated by multiplying the LVOT area by the VTI.

Valvular Area

In a closed fluid system, the amount of flow through one section is the same as the amount of flow through another. This conservation of mass principle is described by the Continuity Equation. Most commonly utilized in the case of aortic stenosis (see Chap. 7—Aortic Valve), the flow through the aortic valve is the same as the flow through the LVOT, so the valve area of the stenotic valve can be determined:

$$A_1 * V_1 = A_2 * V_2 \tag{3.6}$$

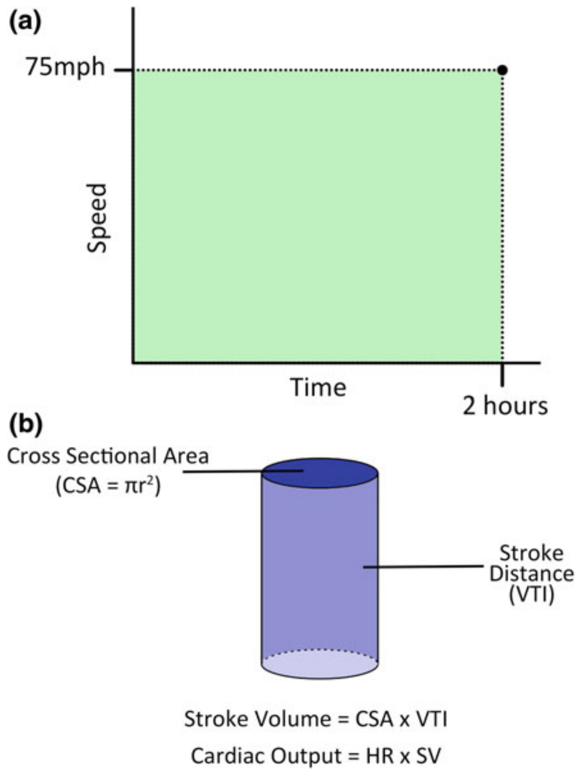

Fig. 3.12 **a** Graph of the speed of a car versus time. The area under the curve which is shaded green demonstrates the distance the car traveled. **b** Depiction of the cross-sectional area of a cardiac structure multiplied by its velocity time integral ("Stroke Distance" will yield a stroke volume). *CSA* Cross-Sectional Area; *VTI* Velocity Time Integral; *HR* Heart Rate; *SV* Stroke Volume

In this example, $A_{\mathbf{LVOT}}$ * $V_{\mathbf{LVOT}}$ **=** $A_{\mathbf{AV}}$ * $V_{\mathbf{AV}}$, where AV is aortic valve and LVOT is Left Ventricular Outflow Tract. One measures the area of the LVOT, and the VTIs for the AV and LVOT (Fig. 3.13a, b). Solving for the area of the AV:

$$A_{\mathrm{AV}} = (A_{\mathrm{LVOT}} * V_{\mathrm{LVOT}})/V_{\mathrm{AV}}$$

Pressure Gradient Estimation

Clinically, practitioners often think in terms of pressure (mmHg) while echocardiography measures velocities. Therefore, a relationship between velocity and pressure is necessary to provide appropriate clinical estimations. The pressure gradient across a valve or orifice can be determined using the modified Bernoulli Equation,

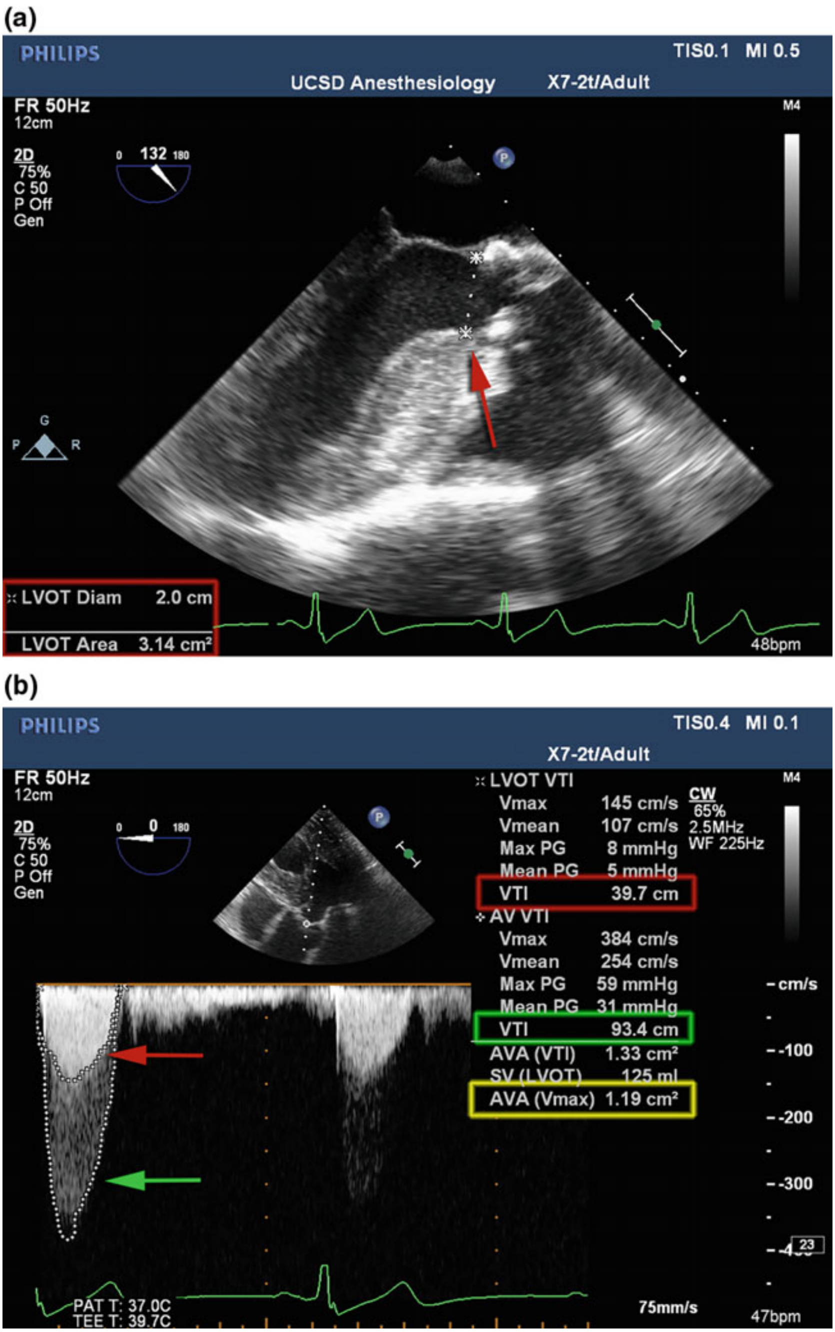

Fig. 3.13 **a** Measurement of the diameter (*red arrow*) of the left ventricular outflow tract (LVOT) using the midesophageal aortic valve long axis view. **b** The "Double Envelope," showing a velocity envelope for the LVOT (*red arrow*, *red box*) and a higher velocity envelope for the aortic valve (*green arrow*, *green box*). Velocity Time Integrals (VTI) are used in the Continuity Equation for calculation of the aortic valve area (*yellow box*)

$$P = 4V^2 \tag{3.7}$$

where P is the pressure gradient, and V is the peak velocity in m/sec. For example, the systolic right ventricular pressure gradient between right ventricle and right atrium can be determined by CWD across the tricuspid valve. The peak velocity of the regurgitant jet, in m/sec, is used in Eq. 3.7. The right ventricular systolic pressure can then be estimated by adding the value of the gradient to the right atrial or central venous pressure (CVP). In the absence of pulmonic valve stenosis, right ventricular systolic pressure is equal to pulmonary artery systolic pressure. Therefore, the application of the modified Bernoulli equation to a tricuspid regurgitation jet in addition to CVP provides an estimation of pulmonary artery pressures (Fig. 3.14).

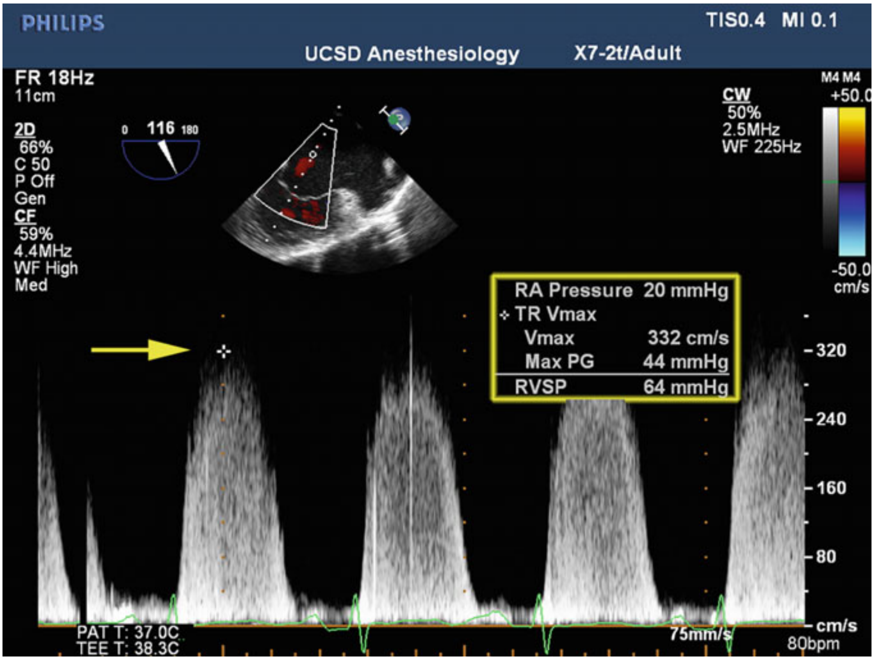

Fig. 3.14 A continuous wave Doppler profile of a tricuspid regurgitation (TR) jet. The right ventricular systolic pressure (RVSP), which is an estimation of pulmonary artery systolic pressure, is determined by applying the modified Bernoulli equation to the peak regurgitant velocity in addition to the CVP (RA Pressure). *RA* right atrial; *Vmax* maximum velocity; *PG* pressure gradient

Summary

Understanding basic principles of sound wave reflection, propagation, and frequency, as well as digital sampling facilitates the effective clinical use of ultrasound technology. These principles can be applied to understand the anatomy and function of the heart, as well as the assessment of blood flow, valve areas, and pressure gradients.

References

1. Brinklov S, Fenton MB, Ratcliffe JM. Echolocation in Oilbirds and swiftlets. Front Physiol. 2013;4:123.
2. Harmon, K. Homing in on Mammalian Echolocation. Scientific American, 2010.
3. Ryckegham, AV. How do bats echolocate and how are they adapted to this activity? Scientific American, 1998.
4. Ulanovsky N, Moss CF. What the bat's voice tells the bat's brain. Proc Natl Acad Sci USA. 2008;105(25):8491–8.
5. Kolarik AJ, et al. A summary of research investigating echolocation abilities of blind and sighted humans. Hear Res. 2014;310:60–8.
6. Schornich S, et al. Psychophysics of human echolocation. Adv Exp Med Biol. 2013;787:311–9.
7. D'Amico A, Pittenger R. A brief history of active sonar. Aquat Mammals. 2009;35(4):426–34.
8. Ludwig G, Struthers F. Considerations underlying the use of ultrasound to detect gallstones and foreign bodies in tissue. Naval medical research institutes reports, 1949. Project 004001 (Report Number 4): p. 20.
9. Singh S, Goya A. the origin of echocardiography. Tex Heart Inst J. 2007;34(4):431–8.
10. Lang RM, et al. Three-dimensional echocardiography: the benefits of the additional dimension. J Am Coll Cardiol. 2006;48(10):2053–69.
11. Aldrich JE. Basic physics of ultrasound imaging. Crit Care Med. 2007;35(5 Suppl):S131–7.
12. Enriquez-Sarano M, et al. Effective mitral regurgitant orifice area: clinical use and pitfalls of the proximal isovelocity surface area method. J Am Coll Cardiol. 1995;25(3):703–9.